Sensor Fusion for Unobtrusive Respiratory Rate Estimation in Dogs

Sensor Fusion for Unobtrusive Respiratory Rate Estimation in Dogs

Christoph Hoog Antink, *Member, IEEE,* Mikko Pirhonen, Heli Väätäjä, Sanni Somppi, Heini Törnqvist, Anna Valldeoriola Cardó, Daniel Teichmann, *Member, IEEE,* Outi Vainio, Veikko Surakka, and Antti Vehkaoja, *Member, IEEE,*

***Abstract*—Respiration is vital to land-dwelling mammals and important information is encoded in the respiratory rate. Objective assessment of the respiratory rate is difficult in dogs, in particular if unobtrusive measurement is desired. The goal of this work was to develop and evaluate a method for unobtrusive sensing of respiratory rate in dogs. For this, the "FlexPock" multisensor system originally developed for unobtrusive estimation of heart rate and respiratory rate in humans via magnetic impedance, accelerometry and optical measurements was used to assess canine respiratory rate. In a proof-of-concept study with 10 healthy dogs of different breeds and sizes, a total of 240 minutes of data was recorded in the phases standing, sitting, lying down, and walking. An algorithm was developed that estimates the respiratory rate by fusing the information from multiple sensors for increased accuracy and robustness. To discard unusable data, a simple yet effective signal quality metric was introduced. Impedance pneumography recorded using adhesive electrodes was used as a reference. Analysis of the raw FlexPock data revealed that magnetic impedance and accelerometry were the best individual sensing modalities and fusion of these data further increased the accuracy. Using leave-one-dog-out cross-validation, the average estimation error was 9.5 % at a coverage of 50.1 %. Strong variation between dogs and phases was however observed. During the walking phase, neither reference nor unobtrusive sensor reported usable results, while the sitting phase exhibited the best performance. In conclusion, fusion of magnetic impedance and accelerometry can be used for unobtrusive respiratory rate estimation in stationary dogs.**

***Index Terms*—Sensor Fusion, Respiratory Rate, Unobtrusive Sensing, Monitoring, Animal Health Management, Dogs**

I. Introduction

RESPIRATION constitutes the external exchange of gases with the ambient atmosphere and is, in the true sense of the word, vital to humans and animals. Changes or obstructions in automated breathing may indicate or lead to health and welfare problems. In dogs, several diseases of, for example lung and heart, can cause difficulties in breathing. Dog breeding has resulted in several breeds with flattened facial and shortened skull anatomy which may cause problematic breathing [1]. At the same time, evaluation of the severity of illnesses or follow-up of treatment efficacy may be hindered, one reason being that communication with the animal is difficult. Therefore, objective and sensitive measurement and analysis of dogs' respiratory rate and effort could help in diagnosis and treatment follow-up.

Panting, i.e. high-frequency breathing with short, quick breaths, occurs due to thermoregulation and during situations of increased oxygen demand, but may also occur as a result of a dog's emotional state [2]. Panting is commonly linked to fear, stress, and pain related behaviors. Excessive panting may indicate an increase in stress hormone (i.e. cortisol) level [3] and has been reported in the context of, for example, kenneling related stress [4], separation anxiety [5], fear of thunder and fireworks [6] and chronic pain [7]. While the respiratory rate could be an objective measure for pain in certain situations, there is no consistent evidence for correlation between respiratory rate and pain, because emotional factors and drugs affect the respiratory rate as well [8]. Although panting is usually associated with negative stress, it may alternatively indicate positive emotional arousal, such as anticipation of a desired reward or reunion with the owner [9], [10]. It has even been suggested that a particular type of breathing rhythm represents laughter in dogs [11]. Hence, continuously measured respiratory rate may be a useful indicator of both the health status and stress or excitement of a dog, for example, when left alone at home or placed in a kennel environment. Respiration information would play an important role in forming a holistic view about the welfare of a dog and in understanding its behavior.

Easy-to-use, unobtrusive methods for everyday physiological monitoring of dogs are receiving increasing interest. Most of the efforts have been put in research of methods for reliable heart rate monitoring. In humans, the electrocardiography (ECG) signal can also be used for respiratory rate estimation, a process known as ECG derived respiration (EDR) [12], which, for example, analyzes the R-peak amplitude variation. Other methods exploit respiratory sinus arrhythmia, i.e. the changes in heart rate in sync with respiration. In dogs, however, this is not possible during panting because the frequency of R-peaks does not fulfill the criteria of Nyquist's theorem, which means that the respiratory rate should be less than half of the heart

C. Hoog Antink and D. Teichmann are with the Chair for Medical Information Technology, RWTH Aachen University, Aachen, Germany. (e-mail: hoog.antink@hia.rwth-aachen.de)

D. Teichmann is also with the Institute for Medical Engineering and Science, Massachusetts Institute of Technology, Cambridge, MA, USA.

M. Pirhonen and A. Vehkaoja are with the Faculty of Medicine and Health Technology, Tampere University, Finland.

H. Väätäjä and V. Surakka are with the Research Group for Emotions, Sociality, and Faculty on Information Technology and Communication Sciences, Tampere University, Finland.

S. Somppi, H. Törnqvist, A. Valldeoriola Cardó, and O. Vainio are with the Department of Equine and Small Animal Medicine, University of Helsinki, Finland.

Manuscript received January 8, 2019; revised March 11, 2019. The work was partially funded by Business Finland as a part of the project Buddy and the Smiths 2.0, grant numbers (1665/31/2016, 1894/31/2016, 7244/31/2016), by the Academy of Finland, grant number 292477 and by the German Research Foundation (DFG), grant number LE 817/26-1.

rate. In fact, the respiratory rate is often even higher than the heart rate during panting.

In clinical practice, animal breathing patterns and difficulties in breathing are usually subjectively assessed in an exercise test by a veterinarian or by owner-directed questionnaires, where the respiration rate is counted manually [13], [14]. However, this subjective assessment is sensitive to errors, and only provide information related to the specific exercise condition. Available methods for objective measuring ventilatory parameters include plethysmography chambers [15] or face masks [16] that both require restraining the dog's movement. For this reason, they are used only for short-time monitoring at the veterinary clinic. In addition to these, Murphy et al. [17] measured dogs' lung volume changes during different body postures with respiratory inductive plethysmography using straps containing coils placed around the thorax and abdomen. In sum, robust, easy-to-use methods for objective measurement of dogs' breathing would still be welcomed, especially in veterinary practice, dog sports, and breathing physiology science.

In this work, we present an approach to estimate respiratory rate in dogs unobtrusively with the wearable multisensor "FlexPock" system. The FlexPock device was originally developed for unobtrusive vital sign estimation in humans, where it is placed in the pocket of a dress shirt [18]. Equipped with optical and mechanical sensors, it requires neither direct skin contact nor adhesive electrodes for its functionality. In humans, respiratory activity can easily be separated from cardiac activity because of its lower frequency. This is however not the case in dogs, where the respiratory rate may vary dramatically and can be higher than the heart rate during panting. Moreover, the dog's fur decreases the signal quality which may impede accurate respiratory rate estimation from a single sensor. Thus, we developed an algorithm for robust respiratory rate estimation which can exploit redundant information from multiple channels via sensor fusion. To evaluate the concept, we conducted a proof-of-concept study with ten healthy dogs of different breeds and sizes. A custom made mobile "SpiritCor9D" device that measures the respiratory rate via impedance pneumography using adhesive electrodes was used as a reference.

II. Materials and Methods

In the following section, the experiment to obtain the data is introduced. Next, the devices used for unobtrusive sensing as well as reference data collection are described. Finally, we present the algorithms to extract respiratory rate and the process of to perform sensor fusion.

A. Data Collection

Ten healthy dogs (9 female, 1 male) participated in the study. Their mean age was 7 years (range from 1 year, two months to 12 years, four months; standard deviation 3 years, 7 months) and their breathing was measured during four conditions: standing, sitting, lying, and walking. Each condition lasted for 1.5 minutes at a time. The conditions were repeated four times in counterbalanced order. Thus, the whole test took 24 minutes. The dogs were handled and instructed by the owner or by one of the researchers. The handler was allowed to give treats to the dog when necessary to keep it motivated for the task. Testing was conducted in an indoor environment at 25° centigrade room temperature. Dogs were not leashed during the data collection. The trials were video recorded to enable post-hoc verification of the annotations. The experimental design was accepted by the Viikki Campus Research Ethics Committee at the University of Helsinki (minutes 2/2018). The basic information of the participating dogs are found in Table I.

TABLE I
Demographics of the participating dogs. Fur type: L = long, S = short, C = curly, TL = two layered, CTB = close to body, F = furry, D = dense, FI = firm.

ID	Breed	Age y, mo	Weight [kg]	Sex	Fur Type
1	Golden Retriever	1, 2	24	F	L, TL, CTB
2	Shetland Sheepdog	5, 1	11	F	L, TL, F, D
3	Australian Shepherd	5, 3	21	F	L, TL, CTB
4	Australian Shepherd	9, 11	22	M	L, TL, CTB
5	Golden Retriever	7, 0	26	F	L, TL, CTB
6	Beauce shepherd	10, 3	31	F	S, TL, FI
7	Beauce shepherd	9, 0	38	F	S, TL, FI
8	Flat Coated Retriever	3, 9	27	F	L, TL, CTB
9	Lagotto Romagnolo	12, 4	15	F	C, TL, F
10	Lagotto Romagnolo	6, 3	13	F	C, TL, F

B. Sensor Systems

1) FlexPock system: The FlexPock device provides three different sensor modalities that are capable of recording a biosignal unobtrusively: Magnetic Impedance (MI) monitoring, reflective Photoplethysmography (rPPG), and Accelerometry [18], [19]. Fig. 1 gives an overview of the FlexPock device.

MI monitoring is based on the fact that each tissue within the body has a different bioimpedance value. In particular, the bioimpedance of lung tissue varies significantly with respiration. Also, as organs move during respiration, the impedance distribution within the body varies. A sensing coil, electromagnetically coupled with the body will measure this variation. The coil excites an alternating magnetic field which induces tiny eddy currents in the dog's body. These eddy currents in turn reinduce a secondary alternating magnetic field which affects the primary one and changes the reflective coil impedance. When the inner bioimpedance distribution changes due to respiration, the size as well as the orientation of the eddy currents will change, both resulting in an observable variation of the coil impedance recorded by the MI device.

rPPG, on the other hand, is based on the fact that biological tissue is an inhomogeneous and anisotropic optical medium. In particular, the absorption coefficient of uncompressed bloodless skin is significantly lower than the one of blood and it also decreases with compression of the skin. The FlexPock device emits light by three LEDs in a triangular arrangement and measures reflected light using a photodiode in the center.

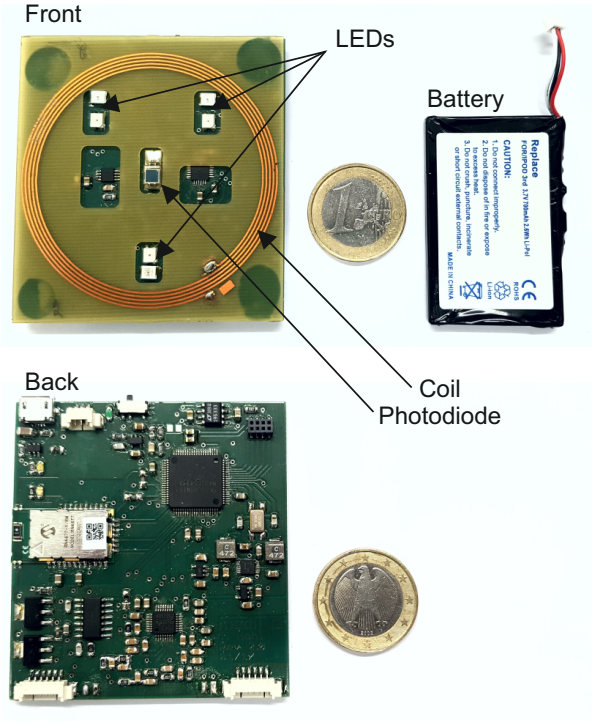

Fig. 1. Photographs of the FlexPock device.

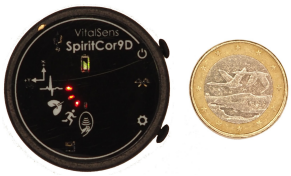

Fig. 2. Photograph of the SpiritCor9D device.

Fig. 3. Placement of devices and electrodes.

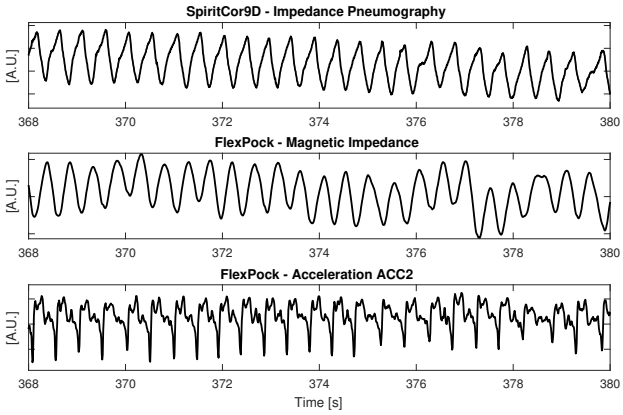

Fig. 4. Example of data recorded with the SpiritCor9D device (row 1, reference impedance pneumography) and FlexPock (row 2, magnetic impedance; row 3 acceleration channel 2).

The amount of reflected light measured by the photodiode will vary with respiration due to three mechanisms: 1) skin perfusion (venous blood return) is modulated by respiration, 2) skin will be compressed or stretched along with expiration and inspiration, 3) the optical coupling between the sensor device and the body surface varies due to motion. In this work, two instances of a rPPG sensor differing in wavelength of the emitted light were used: a near-infrared (wavelength 860 nm) and a red (wavelength 640 nm) version.

Accelerometry is realized with a MPU-6050 motion chip manufactured by InvenSense Inc., San Jose, CA, USA. It obtains the tilting of the device in the x/z plane.

The rPPG and accelerometer are located in the middle of the MI sensor's coil. The device is battery powered and the data is transferred wirelessly via bluetooth to a PC for visualization and storage. All channels were sampled at 100 Hz. More details about the devices hardware setup and circuitry can be found in [18] and [20].

2) Reference data collection: A custom-made physiological monitoring device, SpiritCor9D was used to record the reference data, see Fig. 2:

SpiritCor9D combines measurements of three channels of ECG, one channel of impedance pneumography (IP), 3D acceleration and angular velocity. The IP data is used in the present study for estimating the reference respiratory rate and was recorded at 250 Hz sampling frequency. The data was stored on the internal memory of the monitoring device and later extracted for the analysis performed on a PC computer. Blue Sensor ECG electrodes manufactured by Ambu A/S were used for recording the ECG. The same electrodes also recorded the impedance pneumography data. Model M-OO-S was used with larger dogs and model N-OO-S with the smaller ones (dogs number 2, 9, 10). The IP signal was recorded with electrodes placed behind both front legs. The fur was shaved prior to attaching the electrodes.

The FlexPock device was placed into a frontal pocket sewed inside on a medical pet shirt (MPS-TOP 4in1®, Medical Pet Shirts Europe B.V., Netherlands) and SpiritCor9D into back pocket of the shirt. The placement of devices and electrodes are demonstrated in Fig. 3; an example of data recorded with the FlexPock system and the reference device SpiritCor9D is shown in Fig. 4.

C. Algorithms

1) Reference respiratory rate estimation: Reference respiratory rate was obtained using the IP signal as described above. Impedance of the thorax varies according to breathing but the IP signal also exhibits waveform components originating from the changes of blood volume within the measurement geometry caused by cardiac activity and artifact signal components caused by movements. Due to these sources of disturbance and the fact that a respiration cycle is sometimes ambiguous, we developed the following method for pre-processing the IP signal and obtaining the reference respiratory rate.

The algorithm is based on monitoring the distances of consecutive local maxima in the IP signal and therefore the components caused by the cardiac activity may disrupt the algorithm. To mitigate this effect, adaptive thresholding is used to distinguish the cardiac wave components. The IP signal is differentiated in time and segmented to 1.5 second windows. Signal values above 1.5 or below -1.5 times the RMS value of the respective window are then removed from the non-differentiated signal. Such values were deemed to emerge from cardiac activity. This assumption was visually verified from the respective ECG signal. Removed values are subsequently filled by applying piecewise cubic hermite interpolating polynomials and the IP signal is then smoothed by applying a Savitzky-Golay filter of second order with a frame length of 45 samples. We also apply a 6th order Butterworth high- and low-pass filters in manner of forward-backward filtering with cut-off frequencies of 0.5 Hz and 10 Hz, respectively, to attenuate signal components which may otherwise erroneously be concluded as emerging from respiration. Each local maxima of the IP signal is initially selected by assuming a minimum distance of 50 data points (200 ms) from the next local maxima. When two local maxima are within the minimum distance from each other, the larger one is selected. As a result, we have explicitly ceiled the maximum respiratory rate at 300 breaths per minute (BPM). Moreover, a minimum value in peak prominence, that is, the minimum height of the local maximum from the adjacent local minimum, was specified and local maxima having smaller prominence removed.

Despite the aforementioned IP signal pre-processing steps and rules for selecting the local maxima, postprocessing is still needed to discard erroneous local maxima that are not related to respiration cycles. To accommodate for this, the first derivative of the IP signal is extracted and smoothened by a Savitzky-Golay filter of second order and frame length of 45 samples. Areas formed by each zero crossing of this differentiated signal are then calculated by trapezoidal numerical integration. We assume that in case of true respiration cycles, the areas formed should exhibit similar magnitudes. If the ratio of two adjacent areas is larger than five (or smaller than one fifth), the peak representing the smaller area is removed. Fig. 5 demonstrates the peak rejection, which generally performs well irrespective of dog size or breed. However, in rare instances it was still necessary to manually add or remove peaks to ensure the correctness of the reference.

Following the extraction of peaks, we calculate the peak positions and apply linear interpolation to reconstruct the respiratory rate signal in one-second intervals. Because the respiration rate estimation algorithm used with the FlexPock system reports an average respiration rate for 15 second, an average respiration rate is calculated also for the reference. The IP signal is highly sensitive to movement. During walking, for example, the signal components arising from movement are much stronger than the one caused by respiration. As they fall in the same frequency range, it is difficult to give a reliable reference for the respiration rate. Therefore, a fixed value thresholding was applied in assessing the variance within the accelerometer signal. Portions of the respiration signal were excluded if the corresponding acceleration signal varied over a fixed threshold over a moving window of 1.5 seconds. Besides virtually all the data recorded during walking, this processing step discards part of the data from the transitions between test phases and from giving treats to the dogs.

2) Unobtrusive respiratory rate estimation: Estimation of respiratory rate from the unobtrusive signals is performed using a modification of the "Continuous Local Interval Estimator" (CLIE) algorithm, originally designed to estimate cardiac beat-to-beat-intervals (BBIs) in ballistocardiographic signals [21]. This algorithm has since been used for estimating BBIs in various cardiac signals [22], [23] and is based on the analysis of self-similarity. To estimate local periodicity, i.e. the interval between exactly two events, the lag-adaptive short-term autocorrelation (LASTA) was introduced by Brüser et al. in [21],

$$S_{\mathrm{LASTA}}[\eta] = \frac{1}{\eta}\sum_{\nu=0}^{\eta}\omega[\nu]\omega[\nu-\eta]. \tag{1}$$

Similarly, the lag-adaptive average magnitude difference function (AMDF) is defined as

$$S_{\mathrm{AMDF}}[\eta] = \left(\frac{1}{\eta}\sum_{\nu=0}^{\eta}|\omega[\nu]-\omega[\nu-\eta]|\right)^{-1}. \tag{2}$$

In both equations, a window $\omega[\nu]$ of length L of a signal with discrete time ν is analyzed for a variety of candidate signal shifts η. In this study, L was fixed to 1.3 seconds. Both metrics, LASTA as well as AMDF, produce larger values where the signal exhibits an increased self-similarity, i.e. repeats itself when shifted by η. To increase robustness of the estimation, both measures of self-similarity are fused,

$$S_{\mathrm{fused}}[\eta] = S_{\mathrm{LASTA}}[\eta]\cdot S_{\mathrm{AMDF}}[\eta]. \tag{3}$$

Since self-similarity is in principle modality-independent, the CLIE algorithm allows the fusion of N channels via

$$S_{\mathrm{fused,ALL}}[\eta] = S_{\mathrm{fused},1}[\eta]\cdot S_{\mathrm{fused},2}[\eta]\cdot ...\cdot S_{\mathrm{fused},N}[\eta]. \tag{4}$$

With this expression, the determination of the most probable interval η_{opt} reduces to maximizing equation 4,

$$\eta_{\mathrm{opt}} = \arg\max_{\eta} S_{\mathrm{fused,ALL}}[\eta]. \tag{5}$$

In addition to the most probable interval, the quality metric q is calculated via

$$q = \frac{S_{\mathrm{fused,ALL}}[\eta_{\mathrm{opt}}]}{\sum_{\eta=0}^{L} S_{\mathrm{fused,ALL}}[\eta]}, \tag{6}$$

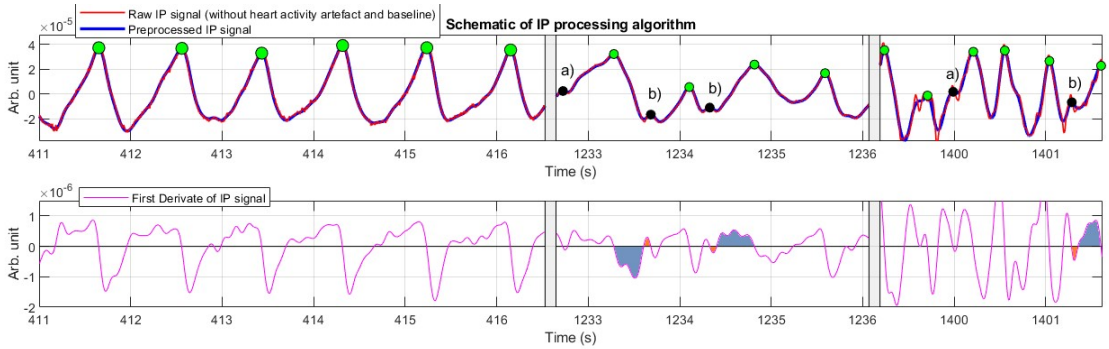

Fig. 5. Example of the peak rejection in IP signal. Extra peaks (local maxima) have been eliminated in the example based on minimum peak prominence (a) and area ratio of subsequent zero crossing (b).

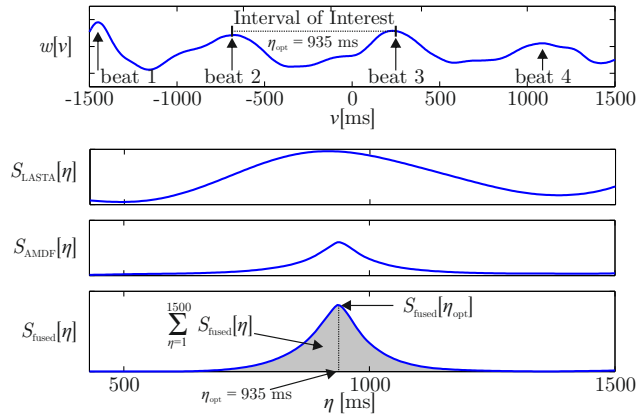

Fig. 6. Principle of the CLIE-Algorithm, modified from [23].

i.e. the ratio of peak height and area under the curve of the fused self-similarity measure. The process is visualized schematically in Fig. 6 for a single channel.

The top row shows the window $\omega[\nu]$ which is three seconds long and contains four events or "beats". Beat 2 and 3 are in the center of the window and the interval between them, i.e. the interval of interest, is 935 ms. Both metrics, LASTA and AMDF show a maximum at η = 935 ms. If the metrics are fused, the maximum becomes more pronounced (bottom panel).

The problem presented in this work, the estimation of respiratory rate from multiple unobtrusive sources, is very similar to the estimation of BBIs in cardiac signals. Instead of measuring the interval between heartbeats, the interval between consecutive breaths has to be determined and inverted to obtain the respiratory rate. In terms of signal waveform, respiratory signals tend to show a smoother behavior than cardiac signals. Thus, a third self-similarity measure of the original CLIE algorithm termed "maximum amplitude pairs" (MAP) [21] is omitted in this implementation as it is sensitive to spikes in the signal. Spikes are characteristic to a variety of cardiac signals, for example the QRS complex in the ECG. However, when analyzing respiratory signals, spikes are more likely to occur due to disturbances rather than physiological events and would thus lead to an increased measurement error in MAP. Finally, the SNR of the measured signals is comparatively low. Thus, rather than calculating intervals on a breath-to-breath basis, we calculate the median value to obtain a robust average breath-to-breath interval within a window of 15 seconds duration,

$$\eta'_{\mathrm{opt}} = \mathrm{median}\left(\eta'_{\mathrm{opt}}\right). \tag{7}$$

By taking the inverse, we get a robust estimation of the respiratory rate within the window,

$$\mathrm{RR}_{\mathrm{est}} = \frac{1}{\eta'_{\mathrm{opt}}}. \tag{8}$$

To determine whether or not the quality of the signal within the window is high enough to allow for reliable respiratory rate estimation, the quality metric q is used in two different ways. For one, the median quality (MQ) is calculated within the 15-second window,

$$\mathrm{MQ} = \mathrm{median}\left(q\right). \tag{9}$$

For another, the normalized median quality (NMQ) is defined as

$$\mathrm{NMQ} = \frac{\mathrm{MQ}}{\mathrm{RR}^2_{\mathrm{est}}}. \tag{10}$$

This metric accounts for the fact that even if the signal is free of noise, the quality metric is lower for signals with lower frequencies and higher for signal with higher frequencies. For both metrics, threshold parameters (t_{MQ} and t_{NMQ}) depending on the use-case can be set.

D. Evaluation

To evaluate the proposed system, the estimated respiratory rate $\mathrm{RR}_{\mathrm{est}}$ was compared to the reference respiratory rate $\mathrm{RR}_{\mathrm{ref}}$ in terms of mean absolute error (in breaths per minute, BPM) as well as relative error (in %). Moreover, the system was evaluated in terms of coverage (in %): The coverage is the fraction of time when the algorithm is able to obtain an estimation of the respiratory rate compared to the total time where a reference respiratory rate is available.

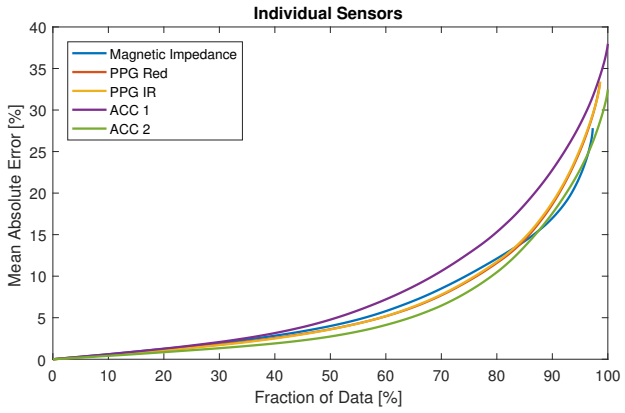

Fig. 7. The mean absolute error of the RR estimate of the individual sensors as a function of the fraction of the data used. The fraction of data is given with respect to the available reference data.

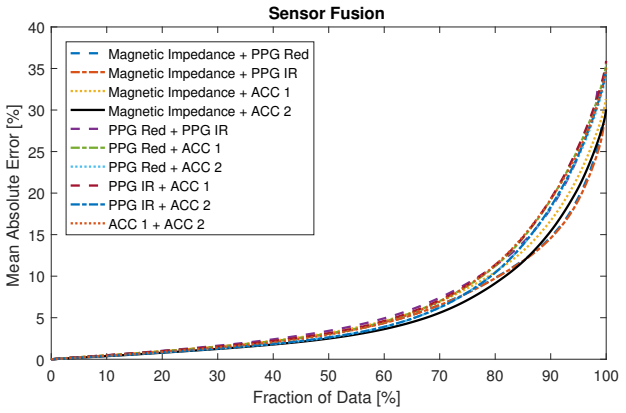

Fig. 8. The mean absolute error of the RR estimate when fusing any two modalities as a function of the fraction of the data used. The fraction of data is given with respect to the available reference data.

III. Results

The analysis of the system is subdivided into two parts. In the first part, the data was analyzed globally. This means that all measurements of all dogs were combined to investigate which individual sensor modality performs best in respiration assessment, how fusion of the modalities improves the estimation, and how the introduced signal quality indices should be used to select the signal segments that provide accurate results. In the second part, to prevent overfitting of the threshold parameters set to the fusion algorithm (t_{MQ} and t_{NMQ}) and to allow for conclusions that can be generalized, leave-one-out cross validation was performed i.e. the parameters were optimized based on the measurements from nine dogs, while the left-out measurement is used for evaluation. Thus, results presented for each measurement were based on optimization with the remaining data.

A. Global Analysis

In the first analysis, the $\mathrm{RR}_{\mathrm{est}}$ was calculated individually from each unobtrusive sensor of the FlexPock device, then compared to the reference and arranged according to the estimation error. With this method it is possible to compare the sensors and select the best ones for the final implementation. Moreover, this naive analysis serves to establish the maximum theoretical performance using the proposed approach. The resulting estimation accuracy obtained with each sensor are displayed in Fig. 7 as a function of the fraction of the data used. Fig. 8 shows the results when any two sensors are fused. Table II presents the optimal relative error for individual sensors and fusion of two at a coverage of 50 %.

As indicated by a visual inspection of the raw signals, it can be seen that all channels contain some sort of respiration related component for most of the time. For example, if the best 50 % of data were known a-priori, all channels would allow the estimation of $\mathrm{RR}_{\mathrm{est}}$ with a relative error of less than 5 %, i.e. with a coverage of 50 %. However, differences among the channels exist. For example, ACC 1 shows the worst performance over the complete data range. On the other hand, the MAE of ACC 2 is the lowest until around 87 % of the data is considered. If more data is used, the MAE of the Magnetic Impedance channel shows the best performance of all individual modalities up until 96 % of the data is used. Fig. 8 and Table II confirm that fusing the Magnetic Impedance channel and ACC 2 gives the best results over all individual sensors and data fractions as well as fusion of any two sensor modalities for data fractions of up to 85 %. An additional inclusion of the optical channels, which have previously been proven useful in human applications for heart rate estimation, did not improve respiratory rate estimation in dogs (results of fusion of more than two modalities not shown for brevity). Thus, in the following, only the Magnetic Impedance channel and ACC 2 were selected to be fused for respiratory rate estimation with the CLIE algorithm.

It can be concluded from Fig. 7 and 8 that accurate

TABLE II
Best achievable relative error for individual sensors and fusion of two for a coverage of 50 %.

Individual Sensors

Modality	Relative Error [%]
Magnetic Impedance	4.00 %
PPG Red	3.62 %
PPG IR	3.59 %
ACC 1	4.77 %
ACC 2	2.74 %

Sensor Fusion

Modalities	Relative Error [%]
Magnetic Impedance + PPG Red	3.07 %
Magnetic Impedance + PPG IR	3.06 %
Magnetic Impedance + ACC 1	3.18 %
Magnetic Impedance + ACC 2	**2.49 %**
PPG Red + PPG IR	3.42 %
PPG Red + ACC 1	3.08 %
PPG Red + ACC 2	2.62 %
PPG IR + ACC 1	3.14 %
PPG IR + ACC 2	2.64 %
ACC 1 + ACC 2	2.96 %

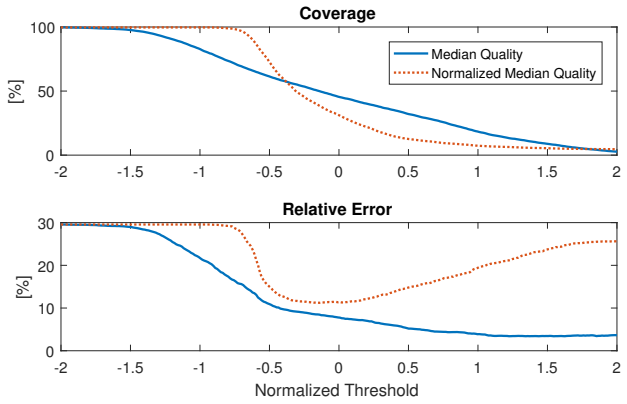

Fig. 9. Dependency of coverage and relative error on the thresholds for Median Quality and Normalized Median Quality, t_{MQ} and t_{NMQ} respectively, if only one parameter is used.

estimation of respiratory rate is possible from certain segments of the unobtrusive data. To find these segments, the quality metrics MQ and NMQ as described above are used. In the first analysis, only those segments were used for which $\mathrm{MQ} > t_{\mathrm{MQ}}$. In the second analysis, only data was used where $\mathrm{NMQ} > t_{\mathrm{NMQ}}$. Results are presented in Fig. 9 in terms of coverage and relative error over a sweep of the normalized thresholds. Normalization was performed by subtracting the mean and dividing by the standard deviation of MQ and NMQ respectively over the complete dataset.

Both parameters show a similar, expected behavior: If each threshold is increased, the coverage decreases monotonically. However, differences exist. While MQ shows an almost linear decrease in coverage, NMQ shows a sharp drop followed by flattening out. Differences are even more pronounced in terms of relative error. Here, only MQ exhibits flat, monotonic behavior. NMQ again shows a sharp drop, but in addition exhibits a minimum at about 0 (i.e. the mean value). If the threshold is further increased, the relative error is increased as well. For both metrics, a tradeoff of coverage and error has to be accepted. In this scenario, if we set a tolerable coverage of, for example, 50 %, an optimum error of 8.5 % can be achieved using a threshold on MQ, whereas a threshold on NMQ leads to an optimal error of 11.7 %.

As both parameters exhibit different behaviors, a combination of both is evaluated in the next analysis. Fig. 10 shows the results if both parameters are used in combination, i.e. data is only accepted if *both* t_{MQ} *and* t_{NMQ} exceed a certain threshold. Using both parameters and a target coverage of no less than 50 %, the optimal achievable error is further reduced to 8.0 %.

B. Cross-Validation Results

Table III shows the cross validation results for all dogs in terms of coverage and error. Here, the thresholds for MQ and NMQ were optimized with a target coverage of no less than 50 % on nine dogs and then used to evaluate the left out recording.

The ten dogs show a strong inter-subject variation in mean RR (from 87 BPM to 205 BPM) as well as a strong intra-

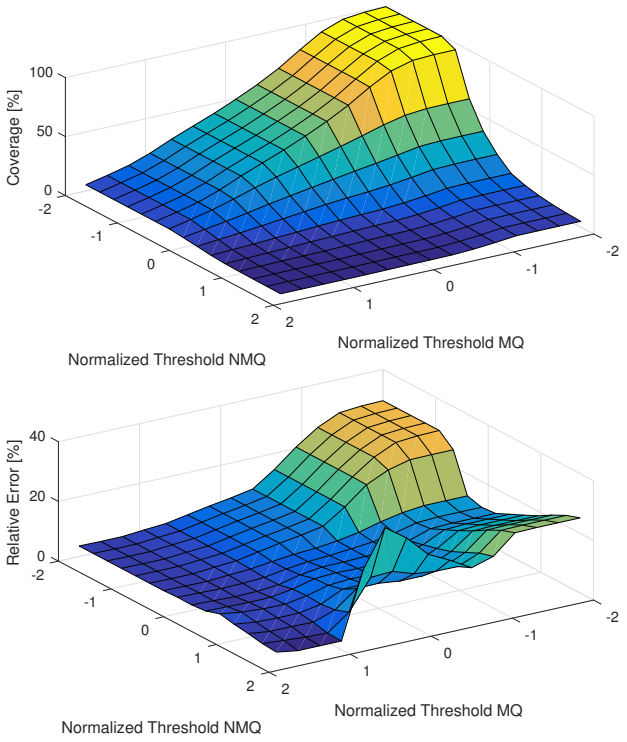

Fig. 10. Dependency of the coverage (top) and relative error (bottom) on t_{MQ} and t_{NMQ} if both thresholds are used in combination.

TABLE III
CROSS VALIDATION RESULTS FOR ALL DOGS IN TERMS OF COVERAGE (COV) AND ERROR. SD = STANDARD DEVIATION.

Dog	Respiratory Rate		Absolute Error				COV
	Mean	SD	Mean		Maximum		
ID	[BPM]	[BPM]	[BPM]	[%]	[BPM]	[%]	[%]
1	193.8	42.1	23.0	13.7	113.5	95.2	52.8
2	87.3	21.2	2.8	6.0	3.6	7.6	0.5
3	204.5	68.2	20.7	10.5	133.5	88.8	19.4
4	124.4	37.0	12.9	9.6	88.3	91.7	34.5
5	154.6	35.5	12.8	11.1	128.8	188.9	81.1
6	161.9	54.7	9.0	7.8	126.5	266.5	73.0
7	136.1	16.5	10.3	8.2	73.7	74.5	91.5
8	214.7	34.5	13.9	7.3	124.5	64.1	70.0
9	191.3	43.9	13.8	8.0	118.3	83.0	11.7
10	196.2	75.4	25.8	12.4	210.4	146.1	67.0
Mean	166.5	42.9	14.5	9.5	112.1	110.6	50.1

subject variability, as the standard deviations of RR within the recordings ranges from 17 BPM to 75 BPM with an average value of 43 BPM. Still our method achieves an average absolute error of only 14.5 BPM, which corresponds to a relative error of 9.5 %, at a coverage of 50.1 %. It is noteworthy, that while the relative error only shows a small variation from 6.0 % to 13.7 % (dog 2 and 1 respectively), the coverage varies from 0.5 % to 91.5 % (dog 2 and 7 respectively). Moreover, comparison of mean and maximum error, i.e. the infinity norm of the error signal, indicates that few but significant outliers are present in most measurements. We observed non-ideal alignment of FleckPock and reference data, which can lead

TABLE IV
CROSS VALIDATION RESULTS SEPARATED BY PHASES. NO VALUE FOR THE ERROR CAN BE COMPUTED IF THE COVERAGE IS ZERO.

	Stand		Sit		Lie Down	
Dog ID	MAE [BPM]	Cov [%]	MAE [BPM]	Cov [%]	MAE [BPM]	Cov [%]
1	13.18	60.49	23.53	58.41	34.33	37.26
2		0.00		0.00	2.84	1.49
3	32.64	24.66	7.49	10.63	12.06	16.13
4	16.06	50.96	10.09	29.28	7.90	17.65
5	11.54	75.24	9.63	82.03	16.92	75.07
6	7.92	68.62	6.30	87.05	14.22	51.45
7	10.66	94.67	6.55	91.10	13.17	83.28
8	16.76	82.32	8.41	76.41	16.70	47.81
9	10.72	10.47	7.36	12.14	20.14	11.15
10	27.23	61.49	9.77	64.14	41.55	46.71
Mean	16.30	52.89	9.90	51.12	17.98	38.80

to outliers when the respiratory rate changes quickly.

For the threshold on MQ, an average value of $6.43 \cdot 10^{-2}$ a.u. was observed with a standard deviation of $7.02 \cdot 10^{-3}$ a.u. over all folds. This corresponds to a relative standard deviation of 10.9 % of the mean. For NMQ, we observed an average value of $2.15 \cdot 10^{-6}$ a.u. with a standard deviation of $2.45 \cdot 10^{-8}$ a.u. This constitutes a variation of only 1.14 % with respect to its mean. Thus, it is interesting to note that while MQ achieves a better individual performance compared to NMQ on the complete dataset (see Fig. 9), NMQ is more robust and the combination of both parameters results in a cross-validated relative respiratory rate error of 9.5 %, which is very close to the error of 8.0 % on the complete dataset (see previous subsection).

As expected, we did not observe correlation between the age of the dog and the coverage or the error. While there was also no correlation between the error and the weight, a significant correlation between the coverage and the weight ($\rho = 0.76, p = 0.01$) was observed. Even if the data of dog number 2, which has the lowest weight and a coverage close to zero, was treated as an outlier and removed, a strong correlation was still observed ($\rho = 0.66, p = 0.05$).

In total, 60 minutes of data were acquired for each test phase. In the three phases "stand", "sit", and "lie down", the reference was available in 48.00, 47.08, and 51.12 minutes, respectively. However, due to intense motion during the "walking" phase, the reference was only available for 0.93 minutes in total. Thus, this phase is excluded in Table IV, which gives the result of the cross validation for all dogs separated by phases. Whenever the coverage is zero for a certain dog and phase, no value for the error is available.

Interestingly, the "sit" phase exhibited the lowest average error of 9.90 BPM at a coverage of 51.12 %. In contrast, the phases "stand" and "lie down" exhibit average errors of 16.30 BPM and 17.98 BPM at coverages of 52.89 % and 38.80 % respectively.

IV. DISCUSSION

The results showed that unobtrusive sensing of respiratory rate in dogs is possible with good accuracy when the dog is not moving by fusing magnetic impedance and acceleration sensing modalities. Overall, a reasonable accuracy was achieved with less than 10 % relative error at a coverage of 50 % with respect to a reference system using impedance pneumography and adhesive electrodes.

While the average values are very promising, we observed large inter- and intra-individual variations. First, we found a significant correlation between the measurement coverage and the weight. In our study, three different harnesses were used depending on the size of the dog and, thus, the contact pressure was adapted. Still, the size of the inductive coil remained constant and may have been less suitable for smaller dogs. Another potential reason could be that the tidal volume of respiration is correlated with the weight of the dog [24], and for this reason larger dogs would produce stronger signals. As a consequence, signals from smaller dogs will also be smaller in amplitude and (assuming constant noise) the signal-to-noise ratio will be decreased as well. The fact that we observed no correlation of error and weight indicates that the proposed method of accepting / rejecting segments of data via thresholds on MQ and NMQ indeed achieved the desired effect. However, the naive global analysis also indicated that when using the CLIE algorithm, at a coverage of 50 % the optimal achievable error would be 2.5 % and if an error of 10 % is tolerable, an optimal coverage of more than 80 % could, in theory, be achieved. Thus, one can think of more complex decision rules that might improve the results further, but which would also require more data for testing to prevent overfitting.

One of the reasons that the coverage was far from a perfect value of 100 % even in the static phases is probably attributed to the fact that data also contained remaining segments during which treats were given to the dog, which were thus not completely stationary. It is interesting to note that the phases "sit" and "lie down" exhibited quite different results, while results for "sit" and "stand" were fairly similar in terms of coverage but not in terms of error. One potential explanation is that during both, "sit" and "stand", the dog had weight on its front legs. As the sensor was placed between them, this results in a relatively constant position for both phases. At the same time, one can speculate that there might have been more motion when the dog was standing compared to when it was sitting and, thus, the error may have increased. When the dog was lying down, the sensor could, for one, shift its relative position and, for another, could also have gotten into contact with the floor, which might have resulted in a restriction of its free motion and thus in a decrease in the acceleration signal quality.

Another important aspect that was not addressed systematically in this study was the influence of the dog's breed on the results. It is interesting to note that the worst results were achieved for the the Shetland Sheepdog, which is not only the smallest dog but also one with a very long, dense fur. We expected some correlation of signal quality and fur properties. Long, dense fur would lead to a larger distance between the

inductive sensor coil and the lung and, thus, to a reduced signal strength. Moreover, coupling with the sensor's accelerometer would also be dampened. On the other hand, the results for the four largest dogs were very promising (average relative error of 8.6 %, average coverage 79 %) although they included two Beauce Shepherd and one Golden Retriever, whose coat is two layered and thick. Thus, we suggest that the influence will not be as significant as the size or the weight.

V. Conclusion

In this work we developed and evaluated a method for robust, precise and unobtrusive sensing of respiratory rate in dogs. The "FlexPock" multisensor system equipped with magnetic impedance, accelerometry and optical measurements was used in a proof-of-concept study with 10 healthy dogs of different breeds and sizes. While the raw data revealed that all channels of the FlexPock system contained respiratory information with varying degrees of usability during static conditions, magnetic impedance measurements and accelerometry provided the most reliable results and the fusion of both channels further increased the accuracy. However, strong variation between dogs and phases was observed, the former being related to significant correlation between the weight of the dog and the coverage. These findings encourage us to future work, which should focus on the increase of motion tolerance and on the thorough analysis of the influence of dog size using a larger sample of test subjects.

References

[1] R. M. A. Packer, A. Hendricks, M. S. Tivers, and C. C. Burn, "Impact of Facial Conformation on Canine Health: Brachycephalic Obstructive Airway Syndrome," *PLOS ONE*, vol. 10, no. 10, p. e0137496, oct 2015.

[2] J. P. Hekman, A. Z. Karas, and N. A. Dreschel, "Salivary cortisol concentrations and behavior in a population of healthy dogs hospitalized for elective procedures," *Applied Animal Behaviour Science*, vol. 141, no. 3-4, pp. 149–157, nov 2012.

[3] M. D. Shiverdecker, P. A. Schiml, and M. B. Hennessy, "Human interaction moderates plasma cortisol and behavioral responses of dogs to shelter housing," *Physiology & Behavior*, vol. 109, no. 1, pp. 75–79, jan 2013.

[4] C. Part, J. Kiddie, W. Hayes, D. Mills, R. Neville, D. Morton, and L. Collins, "Physiological, physical and behavioural changes in dogs (Canis familiaris) when kennelled: Testing the validity of stress parameters," *Physiology & Behavior*, vol. 133, pp. 260–271, jun 2014.

[5] C. Palestrini, M. Minero, S. Cannas, E. Rossi, and D. Frank, "Video analysis of dogs with separation-related behaviors," *Applied Animal Behaviour Science*, vol. 124, no. 1-2, pp. 61–67, apr 2010.

[6] K. Tiira, S. Sulkama, and H. Lohi, "Prevalence, comorbidity, and behavioral variation in canine anxiety," *Journal of Veterinary Behavior*, vol. 16, pp. 36–44, nov 2016.

[7] A. K. Hielm-Bjorkman, E. Kuusela, A. Liman, A. Markkola, E. Saarto, P. Huttunen, J. Leppaluoto, R.-M. Tulamo, and M. Raekallio, "Evaluation of methods for assessment of pain associated with chronic osteoarthritis in dogs," *Journal of the American Veterinary Medical Association*, vol. 222, no. 11, pp. 1552–1558, jun 2003.

[8] K. A. Mathews, M. Sinclair, A. M. Steele, and T. Grubb, *Analgesia and Anesthesia for the Ill Or Injured Dog and Cat*. John Wiley & Sons, 2018.

[9] Z. Y. Ng, B. J. Pierce, C. M. Otto, V. A. Buechner-Maxwell, C. Siracusa, and S. R. Werre, "The effect of dog–human interaction on cortisol and behavior in registered animal-assisted activity dogs," *Applied Animal Behaviour Science*, vol. 159, pp. 69–81, oct 2014.

[10] T. Rehn, A. Beetz, and L. J. Keeling, "Links between an Owner's Adult Attachment Style and the Support-Seeking Behavior of Their Dog," *Frontiers in Psychology*, vol. 8, no. NOV, pp. 1–12, nov 2017.

[11] P. Simonet, D. Versteeg, and D. Storie, "Dog-laughter : Recorded playback reduces stress related behavior in shelter dogs," in *Proceedings of the 7th International Conference on Environmental Enrichment*, 2005, pp. 1–6.

[12] G. B. Moody, R. G. Mark, A. Zoccola, and S. Mantero, "Derivation of respiratory signals from multi-lead ECGs," *Computers in Cardiology*, vol. 12, pp. 113–116, 1985.

[13] L. Lilja-Maula, H. Laurila, P. Syrjä, A. Lappalainen, E. Krafft, C. Clercx, and M. Rajamäki, "Long-Term Outcome and Use of 6-Minute Walk Test in West Highland White Terriers with Idiopathic Pulmonary Fibrosis," *Journal of Veterinary Internal Medicine*, vol. 28, no. 2, pp. 379–385, mar 2014.

[14] S. Pohl, F. S. Roedler, and G. U. Oechtering, "How does multilevel upper airway surgery influence the lives of dogs with severe brachycephaly? Results of a structured pre- and postoperative owner questionnaire," *The Veterinary Journal*, vol. 210, pp. 39–45, apr 2016.

[15] N.-C. Liu, D. R. Sargan, V. J. Adams, and J. F. Ladlow, "Characterisation of Brachycephalic Obstructive Airway Syndrome in French Bulldogs Using Whole-Body Barometric Plethysmography," *PLOS ONE*, vol. 10, no. 6, p. e0130741, jun 2015.

[16] T. C. Amis and C. Kurpershoek, "Tidal breathing flow-volume loop analysis for clinical assessment of airway obstruction in conscious dogs." *American journal of veterinary research*, vol. 47, no. 5, pp. 1002–1006, 1986.

[17] D. J. Murphy, J. P. Renninger, and D. Schramek, "Respiratory inductive plethysmography as a method for measuring ventilatory parameters in conscious, non-restrained dogs," *Journal of Pharmacological and Toxicological Methods*, vol. 62, no. 1, pp. 47–53, jul 2010.

[18] D. Teichmann, D. De Matteis, T. Bartelt, M. Walter, and S. Leonhardt, "A Bendable and Wearable Cardiorespiratory Monitoring Device Fusing Two Noncontact Sensor Principles," *IEEE Journal of Biomedical and Health Informatics*, vol. 19, no. 3, pp. 784–793, may 2015.

[19] S. Leonhardt and D. Teichmann, "Fusing non-contact vital sign sensing modalities - first results*," in *2018 40th Annual International Conference of the IEEE Engineering in Medicine and Biology Society (EMBC)*, vol. 2018. IEEE, jul 2018, pp. 5378–5381.

[20] D. Teichmann, M. Teichmann, P. Weitz, S. Wolfart, S. Leonhardt, and M. Walter, "SensInDenT—Noncontact Sensors Integrated Into Dental Treatment Units," *IEEE Transactions on Biomedical Circuits and Systems*, vol. 11, no. 1, pp. 225–233, feb 2017.

[21] C. Brüser, S. Winter, and S. Leonhardt, "Robust inter-beat interval estimation in cardiac vibration signals," *Physiological Measurement*, vol. 34, no. 2, pp. 123–138, 2013.

[22] C. Hoog Antink, H. Gao, C. Brüser, and S. Leonhardt, "Beat-to-beat heart rate estimation fusing multimodal video and sensor data," *Biomedical Optics Express*, vol. 6, no. 8, pp. 2895–2907, 2015.

[23] C. Hoog Antink, S. Leonhardt, and M. Walter, "Reducing false alarms in the ICU by quantifying self-similarity of multimodal biosignals," *Physiological Measurement*, vol. 37, no. 8, pp. 1233–1252, 2016.

[24] J. Talavera, N. Kirschvink, S. Schuller, A. L. Garrérès, P. Gustin, J. Detilleux, and C. Clercx, "Evaluation of respiratory function by barometric whole-body plethysmography in healthy dogs," *The Veterinary Journal*, vol. 172, no. 1, pp. 67–77, jul 2006.